Journal of Magnetic Resonance **146,** 228–231 (2000)
doi:10.1006/jmre.2000.2140, available online at http://www.idealibrary.com on IDEAL®

A *J*-Multiplied HMQC (MJ-HMQC) Experiment for Measuring $^3J_{HNH\alpha}$ Coupling Constants

Youlin Xia,* Xiangming Kong,* Nancy Ip,† and Guang Zhu*,[1]

**Department of Biochemistry, and †Department of Biology, The Hong Kong University of Science and Technology, Clear Water Bay, Kowloon, Hong Kong*

Received March 20, 2000; revised May 30, 2000

The *J*-multiplied HSQC experiment (MJ-HSQC: S. Heikkinen *et al., J. Magn. Reson* 137, 243 (1999)) amplifies *J* coupling constants *m* times and allows direct observation of the $^3J_{HNH\alpha}$ coupling constants of peptides and proteins (<10 kDa). The drawbacks to this method are line broadening in the f_1-dimension and lower sensitivity. In the *J*-multiplied HMQC (MJ-HMQC) experiment described here, the PEP-HSQC pulse sequence is replaced by a sensitivity-enhanced HMQC section, and the total decay time for the *J*-coupling and the chemical shift evolution is shortened by a period of t_1. This experiment affords narrower linewidth and enhances the sensitivity by 34%, on an average of 105 well-isolated peaks, when compared with the MJ-HSQC experiment. © 2000 Academic Press

Key Words: **NMR; ^{15}N-labeled protein; *J* coupling constant; HMQC.**

The homonuclear three-bond coupling constant ($^3J_{HNH\alpha}$) provides valuable structural information about the backbone dihedral angle, ϕ, in peptides and proteins (*1, 2*). The magnitudes of the *J* coupling constants are correlated with the torsion angles by the Karplus equation (*3, 4*). Accurate measurement of the *J* coupling constants in proteins is fraught with problems that are related to the small size of these couplings relative to the natural proton linewidths.

Several methods (*1, 2, 5–16*) have been developed for the determination of the $^3J_{HNH\alpha}$ coupling constant. Recently, a *J*-multiplied HSQC pulse sequence (*17*) (MJ-HSQC) was described. This method amplifies the *J* coupling constants *m* times and allows direct observation of the $^3J_{HNH\alpha}$ coupling constants of peptides and proteins (<10 kDa). It has better measurement accuracy than COSY and HNHA and very good water suppression properties. The drawbacks to this method are line broadening in the f_1-dimension and lower sensitivity, both of which are caused by the separated evolution periods for *J*-coupling and the chemical shift (*17*). In this paper, we present a *J*-multiplied HMQC (MJ-HMQC) experiment in which these two evolution periods are overlapped by t_1, hence shortening the total evolution time by one t_1 period. In addition, the HMQC method has better relaxation behavior than HSQC. Hence, the MJ-HMQC experiment results in an increase in sensitivity by 34%, on average. Moreover, the spectral linewidths of this experiment are narrower and the water suppression is superior to the MJ-HSQC experiment.

In the MJ-HMQC pulse sequence (Fig. 1), the sensitivity-enhanced HSQC section of the MJ-HSQC is replaced with a sensitivity-enhanced HMQC section (*18–19*). The homonuclear *J*-couplings are present in both the original *J*-coupling period ($(m-1)t_1$), between points *a* and *b*, and in the ^{15}N shift evolution period (t_1) between points *c* and *d*. Thus, the total decay time is reduced from $(m+1)t_1$ in the MJ-HSQC to mt_1 in the MJ-HMQC, with $^3J_{HNH\alpha}$ being amplified *m* times. This modification makes the MJ-HMQC a much more sensitive experiment than the MJ-HSQC experiment.

The evolution of the density operator is

$$\sigma_a = -I_y,$$

where *I* is the amide proton spin operator. During the period of $(m-1)t_1$ between points *a* and *b*, only the ^{1}H homonuclear $^3J_{HNH\alpha}$ coupling needs to be considered, so

$$\sigma_b = I_y\cos[\pi J_{II'}(m-1)t_1] - 2I'_zI_x\sin[\pi J_{II'}(m-1)t_1],$$

where I' is the spin operator of H_α and $J_{II'}$ is the $^3J_{HNH\alpha}$. The homonuclear *J* coupling of protons during the 2τ period between points *b* and *c* can be neglected. Then the proton coherence is transferred into multiple-quantum coherence of the proton and nitrogen through the section between points *b* and *c*

$$\sigma_c = 2S_x\{I_x\cos[\pi J_{II'}(m-1)t_1] - 2I'_zI_y\sin[\pi J_{II'}(m-1)t_1]\},$$

where *S* is the ^{15}N spin operator of the NH moiety. The multiple-quantum coherence is frequency-labeled during t_1 with the chemical shift of nitrogen and modulated with the homonuclear *J* coupling of the protons. The $\pi/2$ pulse just before point *d* transfers the frequency-labeled multiple-quan-

[1] To whom correspondence should be addressed. E-mail: gzhu@ust.hk.

1090-7807/00 $35.00

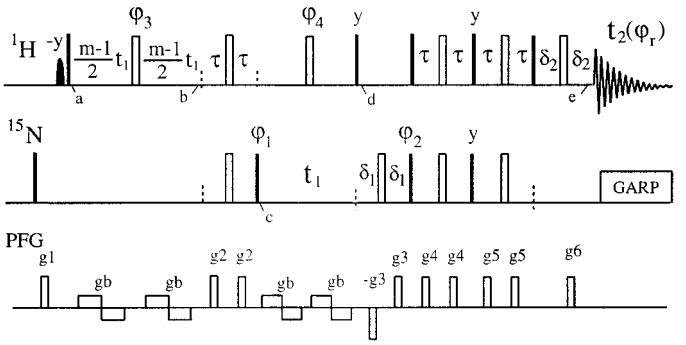

FIG. 1. Pulse sequence for the *J*-multiplied, gradient sensitivity enhanced HMQC. Filled bars and open bars represent 90° and 180° pulses, respectively. Filled shaped pulses are 1.7 ms sinc-modulated rectangular 90° pulses to excite the water resonance selectively. Default phases are x and the experimental recovery delay is 1 s. $\tau = 1/(4^1J_{NH}) \approx 2.7$ ms, δ_1 and δ_2 are g3 and g6 gradient times plus a gradient recovery time of 90 μs. Phase cycling is as follows: $\varphi_1 = (y, -y)$; $\varphi_2 = (-x)$; $\varphi_3 = (x, x, -x, -x)$; $\varphi_4 = 4(x)$, $4(-x)$; $\varphi_r = (x, -x)$. Echo/antiecho selections during t_1 are performed by setting $\varphi_2 = (x)$, and inverting the sign of g3. In order to remove axial peaks, phases of (φ_1 + 180°, φ_r + 180°) are set for every second t_1 increment. The durations and strengths of the gradients are g1 = (1.0 ms, 15 G/cm); g2 = (1.0 ms, 8 G/cm); g3 = (0.5 ms, 25 G/cm); g4 = (0.5 ms, 15 G/cm); g5 = (0.5 ms, 10 G/cm); g6 = (0.1 ms, 0.967*25 G/cm); gb are small bipolar gradients for removing the water radiation damping effect.

tum coherence into an antiphase coherence of the nitrogen with respect to the proton

$$\sigma_d = [S_- e^{i\omega_S t_1} + S_+ e^{-i\omega_S t_1}][-I_z \cos(\pi J_{II'} m t_1) + 2I'_x I_y \sin(\pi J_{II'} m t_1)] \rightarrow - [S_- e^{i\omega_S t_1} + S_+ e^{-i\omega_S t_1}] I_z \cos(\pi J_{II'} m t_1).$$

The antiphase coherence of the nitrogen is then transferred into the inphase coherence of the proton with PEP (Preservation of Equivalent Path)

$$\sigma_e = -[I_- e^{i\omega_S t_1} + I_+ e^{-i\omega_S t_1}]\cos(\pi J_{II'} m t_1) \xrightarrow{t_2} - I_- e^{i(\omega_S t_1 + \omega_I t_2)} \cos(\pi J_{II'} m t_1).$$

Another transient can be obtained through inverting the phase φ_2 and the sign of gradient g3 as

$$\sigma_{e'} = -[I_- e^{-i\omega_S t_1} + I_+ e^{i\omega_S t_1}]\cos(\pi J_{II'} m t_1) \xrightarrow{t_2} - I_- e^{i(-\omega_S t_1 + \omega_I t_2)} \cos(\pi J_{II'} m t_1).$$

A 2D NMR spectrum can be obtained by using the Rance–Kay processing method (*20*). Obviously, the homonuclear J coupling constant ($J_{II'}$) is amplified by m times, but the J coupling time between point a and b only needs to be $(m-1)t_1$, a t_1 period shorter than the MJ-HSQC experiment.

To demonstrate the sensitivity enhancement of the MJ-HMQC experiment over the MJ-HSQC experiment, we applied the 2D MJ-HMQC and its corresponding MJ-HSQC experiments to an ^{15}N-labeled sample of the BC domain (~11 kDa) of the ciliary neurotrophic factor receptor (CNTFR). The protein was dissolved in H_2O at pH 6.3 and experiments were conducted at 30°C on a Varian Inova 500 MHz NMR spectrometer. Figures 2A and 2B show small regions of 2D spectra recorded with MJ-HMQC and MJ-HSQC pulse sequences, respectively. The value of m is 3 in these experiments. Data matrices of 256* × 1024* (* denotes a complex number) in the

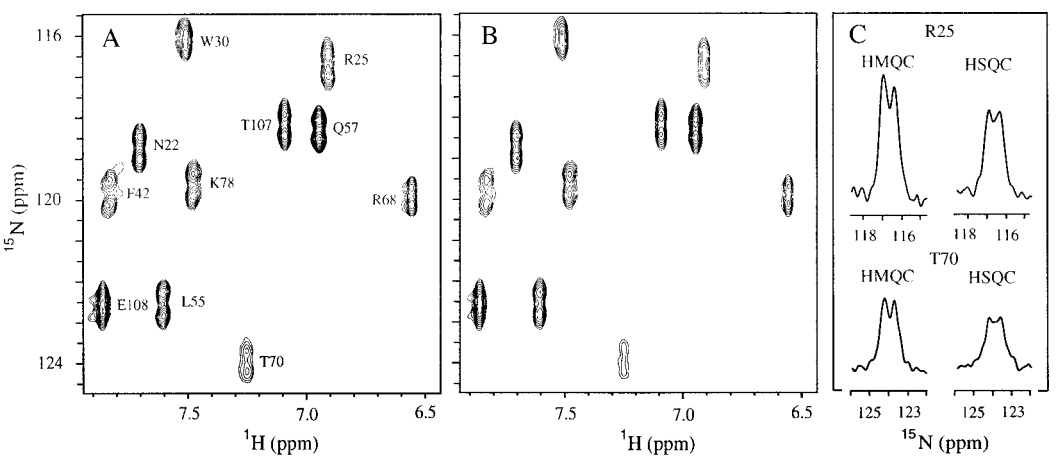

FIG. 2. The comparison of the spectra recorded with the two methods: (A) and (B) small regions of 2D MJ-HMQC and MJ-HSQC spectra, respectively; (C) the corresponding 1D traces of R25 and T70 in (A) and (B). Both spectra were recorded at 30°C on a 1 mM sample of uniformly ^{15}N-enriched BC domain of the ciliary neurotrophic factor receptor (CNTFR) in H_2O at pH 6.3. The lowest contours for spectra (A) and (B) are drawn at the same level. Contours are spaced by a factor of 1.24. The spectra were obtained with identical processing parameters using the nmrPipe software package (*23*).

time domain were acquired for the two spectra, with spectral widths of 1600 and 7000 Hz for f_1 and f_2, respectively. The number of transients for each FID was 32. Spectral matrices of 2048 $\times$ 4096 points for both 2D spectra were obtained with identical processing parameters. Figure 2C shows the corresponding 1D traces of R25 and T70 in Figs. 2A and 2B. Figure 2 clearly indicates that the sensitivity of the MJ-HMQC experiment is increased considerably when compared with that of MJ-HSQC experiment. For 105 well-isolated peaks, the sensitivities of the MJ-HMQC experiment are enhanced by 16 to 61% compared with that of the MJ-HSQC experiment. On average, the sensitivity enhancement of the MJ-HMQC spectrum is 34%. In addition, the splitting of the doublets is clearer and the resonance peaks are sharper, when compared with those of the MJ-HSQC spectrum.

The sensitivity enhancement and line narrowing in the MJ-HMQC experiment are attributable to two reasons. One is that the total decay time for *J*-coupling and chemical shift evolution is shortened by a period of t_1. The other is that the relaxation rate of HMQC is slower than that of HSQC. In the MJ-HMQC and MJ-HSQC experiments, the signal strengths are, respectively, proportional to

$$\exp\left[-\left(\frac{m-1}{T_{2H}}+\frac{1}{T_{2MQ}}\right)t_1\right] \text{ and } \exp\left[-\left(\frac{m}{T_{2H}}+\frac{1}{T_{2N}}\right)t_1\right],$$

in which T_{2H}, T_{2MQ}, and T_{2N} are the transverse relaxation times of ^{1}H, multiple-quantum of ^{1}H and ^{15}N, and ^{15}N respectively. The multiple-quantum transition is not affected, to the first order, by heteronuclear dipolar broadening mechanisms (*2, 21*), and the multiple-quantum T_{2MQ} time can be significantly longer than the corresponding single-quantum T_{2N}. Therefore,

$$\exp\left[-\left(\frac{m-1}{T_{2H}}+\frac{1}{T_{2MQ}}\right)t_1\right] > \exp\left[-\left(\frac{m}{T_{2H}}+\frac{1}{T_{2N}}\right)t_1\right],$$

due to $m-1 < m$ and $1/T_{2MQ} < 1/T_{2N}$. It is worth noting that the effectiveness of the general HMQC experiment over the HSQC experiment is obscured by the homonuclear *J* couplings between H^N and H^α, and thus the spin-locked multiple-quantum coherence is utilized for signal enhancement (*18, 19, 22*). However, the homonuclear *J* couplings between H^N and H^α are just what are needed for measuring the $^3J_{HNH\alpha}$ in the proposed MJ-HMQC experiment. The replacement of HSQC by HMQC is therefore optimal for sensitivity and resolution enhancement.

The correlation of the $^3J_{HNH\alpha}$ values of some residues of the BC domain of CNTFR measured with HNHA (*1*) and MJ-HMQC experiments is shown in Fig. 3. The $^3J_{HNH\alpha}$ values of the HNHA experiment are obtained with Eq. (7.152) from Cavanagh *et al.* (*24*). The *x* coordinate in Fig. 3 is the $^3J_{HNH\alpha}$ value measured with the MJ-HMQC experiment and the corresponding *y*-coordinate is the $^3J_{HNH\alpha}$ value measured with the HNHA experiment. The stars (in Fig. 3) of $^3J_{HNH\alpha} < 8$ Hz are symmetrically distributed near the diagonal, which indicates that the $^3J_{HNH\alpha}$ values of the same residue measured with the two experiments are comparable. However the stars of $^3J_{HNH\alpha} > 8$ Hz are positioned under the diagonal, which indicates that the $^3J_{HNH\alpha}$ values measured with the HNHA experiments are overall smaller than those measured with the MJ-HMQC experiments. If the relaxation effects are not included in the calculation of the *J* values from HNHA experiment, the $^3J_{HNH\alpha}$ values of the HNHA experiment calculated with Eq. (7.152) of Cavanagh *et al.* (*24*) are smaller than their actual values, and the case becomes more and more serious with the increases in the *J* values. This shows that the larger *J* values measured with the MJ-HMQC experiment are more precise than those measured with the HNHA experiment on smaller proteins if the relaxation process is not taken into consideration. The drawback to the MJ-HMQC method is the line broadening in the f_1 dimension. For the protein sample used, *J* values cannot be measured when $J < 3.5$ Hz due to the mergence of the doublets. The low limit of measurable *J* values will be reduced with molecular mass decreasing.

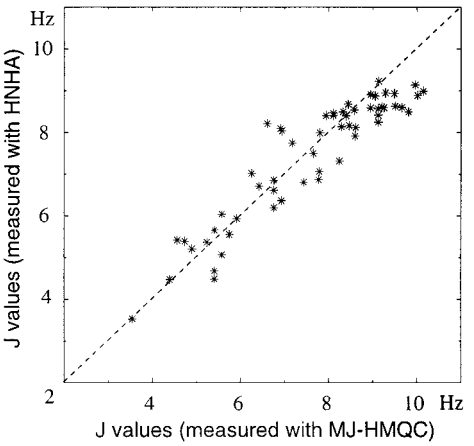

FIG. 3. The correlation of the $^3J_{HNH\alpha}$ values of some residues of the BC domain of CNTFR measured with HNHA (*1*) and MJ-HMQC experiments.

In summary, we have presented a 2D sensitivity-enhanced MJ-HMQC experiment, which can not only amplify the $^3J_{HNH\alpha}$ coupling constants *m* times, but also enhances sensitivity by more than 30% when compared with the MJ-HSQC experiment. Furthermore, small bipolar magnetic field gradients are used in the *J*-coupling and chemical shift evolution times to reduce the effect of water damping and to enhance water suppression. We believe that our experiment is particularly useful for studies involving ^{15}N-labeled peptides or proteins (<10 kDa) because of its superior sensitivity when compared with that of the MJ-HSQC experiment, its good water suppression performance, and its short experimental time (as only a 2D spectrum is required).

ACKNOWLEDGMENTS

This work is supported by Grants HKUST6038/98M and HKUST6199/99M from the Research Grant Council of Hong Kong. We thank Dr. K. H. Sze and Dr. David Smith for critical discussions. The Hong Kong Biotechnology Research institute is acknowledged for the purchase of the 500 MHz NMR spectrometer.

REFERENCES

1. G. W. Vuister and A. Bax, *J. Am. Chem. Soc.* **115,** 7772 (1993).
2. L. E. Kay and A. Bax, *J. Magn. Reson.* **86,** 110 (1990).
3. M. Karplus, *J. Chem. Phys.* **30,** 11 (1959).
4. V. F. Bystrow, *Prog. NMR Spectrosc.* **10,** 11 (1976).
5. S. Ludvigsen, K. V. Anderson, and F. M. Poulsen, *J. Mol. Biol.* **217,** 731 (1991).
6. L. J. Smith, M. J. Sutciffe, C. Redfield, and C. M. Dobson, *Biochemistry* **30,** 986 (1991).
7. D. Neuhaus, G. Wagner, M. Vasak, J. H. R. Kägi, and K. Wüthrich, *Eur. Biochem.* **151,** 257 (1985).
8. M. Billeter, D. Neri, G. Otting, Y. Q. Qian, and K. Wüthrich, *J. Biomol. NMR* **2,** 257 (1992).
9. D. Neri, G. Otting, and K. Wüthrich, *J. Am. Chem. Soc.* **112,** 3663 (1990).
10. H. Kuboniva, S. Grzesiek, F. Delaglio, and A. Bax, *J. Biomol. NMR* **4,** 871 (1994).
11. R. Weisemann, H. Rüterjans, H. Schwalbe, J. Schleucher, W. Bermel, and C. Griesinger, *J. Biomol. NMR* **4,** 231 (1994).
12. G. T. Montelione and G. Wagner, *J. Am. Chem. Soc.* **111,** 5474 (1989).
13. J. Cavanagh, W. J. Fairbrother, A. G. Palmer, III, and N. J. Skelton, "Protein NMR Spectroscopy," Academic Press, San Diego (1996).
14. J. D. Forman-Kay, A. M. Gronenborn, L. E. Kay, P. T. Wingfield, and M. Clore *Biochemistry* **29,** 1566 (1990).
15. V. V. Krishnamurty, *J. Magn. Reson.* **B113,** 46 (1996).
16. V. V. Krishnamurty, *J. Magn. Reson.* **A121,** 33 (1996).
17. S. Heikkinen, H. Aitio, P. Permi, R. Folmer, K. Lappalainen, and I. Kilpeläinen, *J. Magn. Reson.* **137,** 243 (1999).
18. G. Zhu, X. Kong, and K. Sze, *J. Magn. Reson.* **135,** 232 (1998).
19. X. M. Kong, K. H. Sze, and G. Zhu, *J. Biomol. NMR* **14,** 133 (1999).
20. L. E. Kay, P. Keifer, and T. Saarinen, *J. Am. Chem. Soc.* **114,** 10663 (1992).
21. A. Bax, L. E. Kay, S. W. Sparks, and D. A. Torchia, *J. Am. Chem. Soc.* **111,** 408 (1989).
22. S. Grzesiek and A. Bax, *J. Biomol. NMR* **6,** 335 (1995).
23. F. Delaglio, S. Grzesiek, G. Vuister, G. Zhu, J. Pfeifer, and A. Bax, *J. Biomol. NMR* **6,** 277 (1995).
24. J. Cavanagh, W. J. Fairbrother, A. G. Palmer, III, and N. J. Skelton, "Protein NMR Spectroscopy, Principles and Practice," pp. 526, Academic Press, San Diego (1995).